ITU A|Z • Vol 22 No 3 • November 2025 • 795-813

# A multi-objective optimized framework for window integrated photovoltaic systems toward occupants' comfort and energy-saving in office buildings

**Narges BARZANOUNI**[1*], **Hamid Reza HAGHGOU**[2]
[1] mlk.barzanouni@gmail.com • Department of Architecture and Urban Design, Faculty of Architecture and Urban Planning, Art University, Tehran, Iran
*ORCID: 0000-0002-0346-6979*
[2] hrhaghgou@yahoo.com • Materials and Energy Research Center (MERC), Tehran, Iran
*ORCID: 0009-0000-2412-3126*

* *Corresponding author*
*Received: December 2023 • Final Acceptance: May 2025*

**Abstract**
Window Integrated Photovoltaic systems have significant potential for improving building energy saving and occupant comfort, but their impact on visual and thermal environments are not widely studied. This study aims to develop design guidelines for photovoltaic-integrated windows in office buildings, optimizing both energy performance and occupant comfort. A prototypical south-face office room was simulated in various regions at latitudes 34°-37°, representing semi-arid, arid, warm temperate, and cold-semiarid climates, following the Köppen Climate Classification. The simulations assessed different Window-to-Wall Ratios (WWR) and Photovoltaic (PV) Panel-to-Window Ratios (PWR) to determine the most effective configurations. Results indicate that, in arid climates, large PV-integrated windows, as introduced in this study, achieve higher energy saving and visual and thermal comfort compared to conventional clear windows. The best configuration is equal to 50% WWR, 80% of which is a transparent PV layer.

**Keywords**
Energy saving, PV-to-window ratio, Thermal comfort percentage, Useful daylight illumination, Window-to-wall ratio.

*doi: 10.58278/0.2025.113*

## 1. Introduction

Energy consumption has increased dramatically, a vast majority of which is provided by fossil fuels (Ghosh et al., 2019). About 60% of electricity is generated by fossil fuels (The International Energy Agency [IEA], 2022), meanwhile, the year 2020 saw a pronounced decrease in fossil fuel production compared to the preceding year, 2019 (IEA, 2021). In addition, today, the energy use of buildings (heating, cooling, lighting, and equipment) contributes to almost 28% of worldwide carbon dioxide emissions (Gentile et al., 2022). To decrease $CO_2$ emissions and building energy use, it is important to apply renewable energy resources that are more effective as well as manage building energy requests (Chae et al., 2014). The primary types of technologies used for solar electricity generation are Photovoltaic and solar-thermal power.

In integrated photovoltaic systems, Photovoltaic technologies are integrated into conventional building materials like roofs, skylights, or facades to generate electricity (Parida et al., 2011). Windows integrated with photovoltaic cells function similarly to conventional windows and at the same time generate electricity. Many studies have shown that their energy performance is good (Kuhn et.al, 2021; Bakmohammadi & Noorzai, 2021). By installing semi-transparent Building-Integrated Photovoltaic Windows, we reduce our environmental footprint and enhance our society's sustainability (Liu et al., 2019).

Window integrated with PV includes a wider range of different types and each of which needs many sensitivity analyses as many factors affect their performance, so on these topics, research has yet to be thoroughly explored. A key decision in passive building design in a particular climate is the selection of a suitable glazing area for architectural geometry (Liu & Wu, 2022). With appropriate customization, many barriers to BIPV adoption can be overcome, such as aesthetics, architectural integration, and performance (Attoye et al., 2017).

Studies such as Hu et al. (2023), Sun et al. (2020), and Liu et al. (2019) prioritize daylighting and glare control in their investigations, showing how PV windows improve visual comfort. In contrast, Kim et al. (2023), and Chen et al. (2019), focus more on energy metrics, like NZB buildings potential and energy consumption. Their studies reveal that while energy generation from PVs is beneficial, careful consideration of factors like WWR, PV coverage, and type of PV technology can enhance both comfort and energy outcomes. Thei studies demonstrate the multidimensional value of PV-integrated windows.

Hu et al. studied Cadmium Telluride (CdTe) photovoltaic windows effects on the daylight environment of the indoor spaces. Experiments in a test room were conducted to evaluate three indoor daylight factors, visible transmittance ($t_{vis}$), solar heat gain coefficient (SHGC), and glare index of the windows. It was found that by maintaining a satisfactory level of daylighting, the window can effectively reduce solar heat gain and glare, also windows integrated photovoltaic can contribute to energy savings and improve daylight conditions indoors. Compared with conventional windows the PV windows are more effective in reducing SHGC and glare (Hu et al., 2024).

Kim et al., (2023), proposed a window integrated with third-generation PV panels. The system was analyzed technically and economically for a residential building and the feasibility of the system was assessed to contribute to achieving NZE buildings. In terms of technical performance, it evaluates the energy generation potential of the integrated PV system. This involved considering architecture variables, such as region, building orientation, window size, and building type, as well as the type of PV panels used. On the economic front, it conducted a Life Cycle Cost (LCC) analysis to assess the economic performance of the integrated PV system. These indicators provide insights into the economic feasibility and cost-effectiveness of the window integrated PV system (Kim et al., 2023). Newer generations of photovoltaic (PV) panels, specifically transparent thin-film panels, can overcome the limitations of traditional silicon-based solar cells. Furthermore, to be lightweight, flexible, and semi-transparent, they can be used in windows and other

building surfaces. PV panels based on third-generation silicon are typically more efficient and cheaper than silicon-based PV panels.

In the research done by Sun et al., 2020, various types of photovoltaics integrated with south-facing windows of an office were specified to be examined under different WWRs[1]. Dynamic simulations using RADIANCE were conducted to analyze the Useful Daylight Illuminance, UDI[2], daylight Uniformity Ratio (UR), and Daylight Glare Probability (DGP). The comparison of conventional double-glazed windows and PV windows under different climates (Shanghai, Harbin, and Guangzhou), proved that all the tested PV windows demonstrate an improvement in daylight performance, in particular, a significant improvement in glare perception. Additionally, the study establishes criteria thresholds for the effectiveness of the daylight environment, where certain PV windows qualify as "Best" or "Good" practice based on the percentage of working hours with imperceptible or weaker-than-perceptible glare. "Good practice" defines as having a UR that exceeds 0.3, as recommended by BREEAM. It shows that tested PV windows reduce the rate of glare and the simulations provide insights into the potential of different PV window prototypes to improve daylight availability and uniformity (Sun et al., 2020).

Liu et al., (2019), explored different types of PV layers used in semi-transparent PV windows. The PV layers discussed various configurations of CdTe solar cells integrated into glazing systems with different transparencies (20%, 30%, 40%, and 50%). The goal was to investigate daylight performance of the windows. For daylight quantity evaluation UDI were used and for daylight quality evaluation DGP, Illuminance Uniformity (UO), Correlated Color Temperature (CCT), and Color Rendering Index (CRI) were used. The paper mentioned the presence of semi-transparent PV windows affects the indoor thermal environment by allowing solar radiation to penetrate through gaps between solar cells. This can contribute to passive heating, which influences the overall thermal comfort within the building. While the paper primarily addressed the visual and daylighting aspects, it acknowledged the importance of thermal performance as part of a holistic evaluation of PV window integration. The paper showed that CdTe PV windows offer significant improvements over conventional clear double glazing in terms of daylight performance. They, also, provide better daylight distribution, reduce glare, and maintain high color quality of transmitted light (Liu et al., 2019).

Chen et al., 2019, compared energy performance of a room using ordinary windows and of a room with STPV windows. The c-Si PV windows with crystal silicon arrangement were developed that consisted of three parts, a translucent photovoltaic glazing layer, a conventional transparent glass, and an air gap between them. The results indicated that the room with photovoltaic (PV) windows experiences higher lighting energy consumption compared to the room with regular windows, due to the obstruction caused by the c-Si photovoltaic modules. However, the energy consumption for air conditioning decreased. Although the electricity generated by the PV windows cannot cover all the building's energy needs, it can offset the increased lighting energy consumption. The study of the room with semi-transparent photovoltaic (STPV) windows, where 85% of the surface is covered by PV cells, revealed that energy consumption peaks when the window-to-wall ratio (WWR) is 0.08 and is lowest when the WWR is 0.83. As the WWR increases, lighting energy consumption decreases while cooling energy consumption rises due to more solar radiation entering the room. However, this also leads to higher heating energy consumption because the heat loss through the window surpasses the solar heat gain. Additionally, as the active PV area increases, PV power generation also increases. Consequently, the total annual energy consumption decreases with higher WWR due to the balance between the reductions and increases in energy consumption and the energy generated. It is also important that the conductivity of the tested

window is almost 0.04 $W \diagup m.K$. The study investigated different PV coverage with varying WWRs too. For a small WWR, the total energy consumption minimizes when the PV cell coverage ratio is 73%. As coverage increased, cooling energy decreased, power generation increased, but heating and lighting energy increased. As the WWR increased, the optimal PV cell coverage ratio shifted to higher values. This is because with larger WWR, the reduction in cooling energy consumption and the increase in power generation from the PV cells become more dominant factors. The study concluded that for a south-facing window in southwest China, the lowest energy consumption occurs with a WWR of 0.83, 87% PV cell coverage, and an air gap depth of 9 mm (Chen, et al., 2019).

Cannavale et al., 2017, studied the influence of BIPV windows on visual comfort and energy performance. It is the first study that is considered the electricity production potential of PV integrated windows and their visual comfort advantages. Their research illustrates that integrating PV cells in small windows can increase UDI compared to clear windows. PV integration to the large windows leads to more electricity generation (Cannavale, et al., 2017). The architecture studio at the Izmir Institute of Technology encounters difficulties related to the distribution of daylight and glare issues. Taser and Kazanasmaz, (2023), explored the use of solar cells installed on windows within this studio and discovered that they enhance visual comfort as well as the overall daylight performance. Crystalline silicon cells can manage a substantial portion of the lighting demands throughout various seasons and boost energy efficiency (Taser & Kazanasmaz, 2023).

Though electrical power systems can be generated on-site, PV windows and their impacts on the daylight and thermal environment have not been extensively studied. In a review article on BIPV windows developments and researches (Yu et al., 2021), it is indicated that a few studies are concentrated on the impact of BIPV windows on energy performance and it is excellent. This study limited the effects of PV-integrated windows on heating/cooling and lighting energy consumption and electricity generation. While, the transmitted light and heat from the windows can significantly affect the visual and thermal comfort in a room. According to this review paper, a-Si cells are the widest PV cells investigated by previous literature. They emphases the importance of climate conditions on the BIPV windows, because different angle of incidence will result in different thermal and lighting performance of windows.

As regards all literature reviews mentioned above, many studies have done to evaluate the performance of BIPV windows, but none of them consider thermal and visual occupant comfort parallel to their effect on energy demand. Among all studies investigating BIPV windows, there are a few that investigates thermal comfort and daylighting. Most of them are concentrated on the energy demand (Kim et al., 2023; Gao et al., 2022; Chen et al, 2019; Do et al, 2017; Chae et al, 2014; Samanoudy et al, 2024; Yu et al, 2021). There is research analyzed daylight performance (Liu et al, 2019; Sun et al, 2019; Cannavale et al, 2017); or the outdoor microclimate (Chen et al., 2021). However, Chen et al., 2019, investigated BIPV windows to find the best WWR which results in the least energy consumption, this study achieves the best configuration in smaller window size that can cause Economic savings. Chen et al., 2019, results that the optimal PV integrated windows (0.83 WWR and 0.87 PV covered area) leads to more energy saving, while the results of this study reach to the optimum figures with smaller window area. Figure 4 illustrates that when WWR is 40, 50, or 60 %, the amount of F, the criteria showing the highest thermal/visual comfort and energy saving, reaches 120-140 by 60% PV covered area of it. While when WWR is 80%, F reaches to 120-140 by more than 70% PV covered area. This is the first research considers energy saving of PV integrated windows, while concentrates on their visual and thermal effects.

The thermal, lighting, and electrical performance of BIPV windows requires more study, especially because

of the relation between Vt, SHGC and electricity generation. A comprehensive multi-objective building simulation model has been developed to estimate the performance of the BIPV windows under different climatic conditions.

Window-integrated photovoltaic systems represent a promising solution that serves the dual purpose of generating on-site electricity while performing as conventional glazing. Former studies have demonstrated the high energy performance of these semi-transparent PV windows. Still, most previous exploration has only optimized one or two parameters. This study, Specifically, investigates the effects of sunlight to better understand its impacts on occupant comfort. The model analyzes combinations of different PV-to-clear window ratios and window-to-wall ratios for locations in climate zones that have not been considerably studied. By optimizing useful daylight situations, thermal comfort, and energy effectiveness all-together, this work provides a more holistic assessment of PV window configurations. The results aim to offer novel perspectives to fully harness their potential for reducing not only building energy use but also carbon emissions.

The uniqueness of this research, also, is that it investigates the non-visual effects of sun rays as well as the visual ones to exploit the capabilities of solar power fully. Considering the specification of the glazing system, like $t_{vis}$ and SHGC, it achieves the highest percentage of thermal comfort while ensuring higher useful daylight illuminance and optimizing the building's energy consumption. It analyzes a combination of different percentages of PV-to-clear-window ratios as well as window-to-wall ratios that are set up for different cities located in different climate zones that have not been studied before. In the current study, more than one city is examined. The cities located in the high latitudes are chosen and the results can be applied for constructions in all similar regions. The data and results are helpful for designers and decision makers. No decision-making approach was employed to find the framework before this workflow.

In this study, a window that uses second-generation PV cells, thin-film technologies, is proposed to investigate its effects on energy demand while occupant comfort is satisfied. First, the methodology section explains the model description, and different types of the PV to window ratios and elaborates on the mathematical model of the PV window concerning the characteristics of photovoltaic glass like optical and thermal mechanisms. Calculating electricity generated by PV. After that, the definition of discrete sensors, performance indicators, thermal and visual comfort model are explained. Then, an assessment of the geographical locations and meteorological data is presented in the Climate section. Simulation Model and applying cooling, heating, and artificial lighting systems for the building, and parametric study procedure and fitness function are presented, after all. The remainder of the paper is structured as follows: in the Result and Discussion, a comparison of energy consumption among different climates was conducted to provide a better overview about the selected climates. the result of the fitness function to find the optimized solution is explained here to introduce the best configuration of the PV integrated window that ensures higher occupant comfort whilst leads to less energy consumption. Finally, the payback of the BIPV glazing system is calculated. This last part provides justifiable reasons to show that PV integrated windows using a-Si cells not only help sustainability built operationally and aesthetically, but also are efficient economic-wise. A summary of conclusions drawn from the present study is outlined in the last section.

## 2. Method

A hypothetical model for the office room was chosen. A south-faced window of the room was investigated to find optimum results of energy demand, thermal comfort, and daylight illuminance. The effects of total window-to-wall ratio and the PV-integrated window share of the window are investigated. The tested PV window includes five different window-to-wall ratios (WWR), 20%, 40%, 50%, 60%, and 80%, and seven different PV-to-window

ratios (PVWinR), 20%, 30%, 40%, 50%, 60%, 70%, and 80%. The methodology is detailed in sections 2.1 to 2.9. Each step, from the initial geometry (2.1) to the final fitness function interpretation (2.9), contributes to the comprehensive analysis. A workflow diagram (figure 1) provides a visual overview of these steps. After finding the best configuration of the window, the payback of a PV integrated window is calculated to justify its usage in the buildings. The payback is calculated using Simple Payback Period method.

### 2.1. Climate condition

Iran has more energy consumption than the world by an average of 64% (Nasrollahzadeh, 2021). The total final energy consumption in Iran during the years 1967–2006 shows an upward trend. Its energy consumption is much more than the developed countries (Roshan, et.al, 2012). In Iran, 25% of electricity usage in offices is the result of artificial lighting. Iran is chosen because it has a high daylight availability with a great potential to use solar energy (Global Solar Atlas, 2019).

This study investigates semi-arid, arid, warm-temperate, and cold-semi-arid climates (table 5). The simulations are carried out for 4 cities of Iran, a semi-arid climate ("BSh", Tehran with a latitude of 35.4 degrees, Iran), an arid climate ("BWh", Sabzevar with a latitude of 36.1 degrees, Iran), a warm temperate climate ("Cfa", Rasht with a latitude of 37.2 degrees, Iran), and a cold-semiarid climate ("BSk", Tabriz with a latitude of 38.8 degrees and Kermanshah with a latitude of 34.2 degrees, Iran) following the Köppen Climate Classification to achieve a framework. These cities were chosen based on geographic location and their latitudes. The weather data files are from climate.onebuilding.org. This site updated the weather information and included generated files using 2007 to 2021 data. The annual direct normal and diffuse horizontal radiation is calculated through the weather file data.

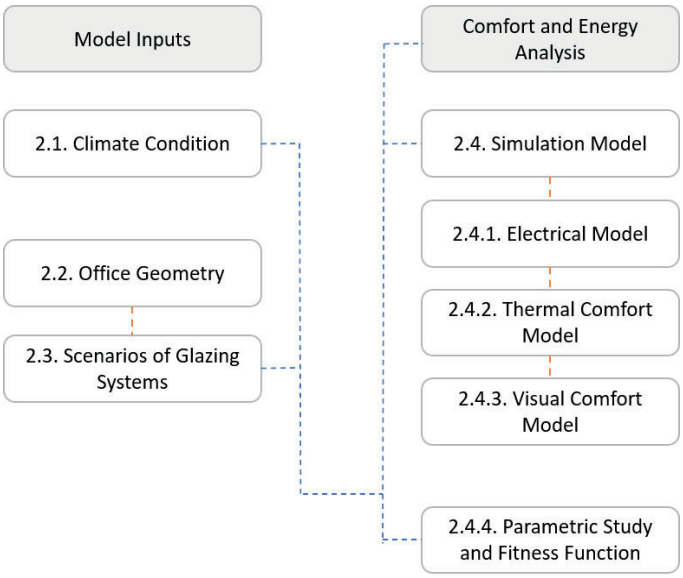


***Figure 1.*** *Overview of methodology steps.*

***Table 1.*** *Weather Statistics File (https://climate.onebuilding.org).*

| Reference | Cold-semiarid | subtropical hot-steppe | subtropical hot-desert | subtropical humid-mild | Cold-semiarid |
|---|---|---|---|---|---|
| Site:Location | Kermanshah-BK | Tehran-Mehrabad | Sabzevar AP KV | Rasht.Intl.AP GI | Tabriz.Intl.AP EA |
| Latitude | {N 34° 19.02'} | {N 35° 41.34'} | {N 36° 10.08'} | {N 37° 19.50'} | {N 38° 8.04'} |
| Longitude | {E 47° 4.98'} | {E 51° 18.78'} | {E 57° 35.70'} | {E 49° 36.36'} | {E 46° 14.10'} |
| Elevation above sea level (m) | 1295 | 1208 | 908 | 12 | 1359 |
| Maximum Dry Bulb Temperature (°C) | 37.° Occurs on Jun. 18 | 41.° Occurs on Jun. 29 | 41.° Occurs on Jun. 7 | 36.° Occurs on Aug. 20 | 39.° Occurs on Jul. 18 |
| Minimum Dry Bulb Temperature (°C) | -20.° Occurs on Jan. 12 | -3.° Occurs on Jan. 30 | -5.° Occurs on Dec. 8 | -1.° Occurs on Jan. 11 | -13.° Occurs on Jan. 7 |
| Direct Normal Radiation {kWh/m2} | 2400 | 2444 | 2402 | 1660 | 2350 |
| Global Horizontal Radiation {kWh/m2} | 2015 | 2010 | 1975 | 1541 | 1898 |
| Köppen Classification | BSK | BSh | BWh | Cfa | BSk |

### 2.2. Office geometry

The width, length, and height of the prototypical office room are 4.5, 6, and 3.5 meters, respectively (figure 2). Only the boundary condition of the south wall is simulated outdoors, because of its favorable conditions for PV applications (Somasundaram et al., 2020) with a U value of 0.42 (W/m^2.K). No obstructions outside the office, such as surrounding buildings and vegetation and no frame for the window are assumed.

The window is split into two parts horizontally, a PV window and a clear window to investigate the optimum manner of a window combination. The upper part of the window is assigned as the PV window. The WWRs and PV-integrated to-window ratios (PVWinR) selected as variants and 35 configurations examined (Table 2). we included this boundary to investigate a wider range of potential scenarios.

### 2.3. Scenarios of glazing systems

The glazing system integrates a PV layer while a 12-millimeter air gap and clear glasses are added to its interior side to minimize the U-value of the window. So, the transparent PV window comprises a triple-glazed configuration where a solar cell layer is encapsulated between two transparent glazing panes (figure 2). This research investigation treats the PV layer as a semi-transparent module incorporating amorphous silicon (a-Si) solar cells, the second-generation thin-film solar cell technology. The low-E layer could cause a reduction in visible transmittance however, most modern Low-E coatings are designed to provide a good balance between energy consumption and natural daylighting. Then, his assembly is divided into two sections: one part is a standard triple-glazed configuration with higher solar radiation transmittance ($t_{sol}$), visible light transmittance ($t_{vis}$) and solar heat gain coefficient (SHGC), while the other section incorporates the PV glazing with similar U-factors. The effects of the frame on thermal and visual performance are not considered in this study. This layout allows for a comparative assessment of performance between conventional glazing and PV glazing options. Table 3 outlines the layer-by-layer characteristics of the glazing systems that were modeled in LBNL Window Software to calculate their visual and thermal characteristics. The characteristics of the modeled glazing systems is shown in Table 4. As Table 4 shows, U-factor of both PV-window and clear window are nearly identical and their SHGC, $t_{vis}$, and $t_{sol}$ are different. The findings of this study aim to identify optimal configurations that maximize useful daylight, thermal and visual comfort, and electricity generation.

***Table 2.*** *Room dimensions and the rate of increment of the window.*

| Dimensions | Design range | Interval |
|---|---|---|
| Room Width (m) | 4.5 | constant |
| Room Length (m) | 6 | constant |
| Room Height (m) | 3.5 | constant |
| PV-Window to Total Window Ratio (PVWinR) | 20%-80% | 10% |
| Window-to-Wall Ratio | 20%-40%-50%-60%-80% | |

***Table 3.*** *Glazing system specifications.*

| | Layer | Thickness (m) | Conductivity (W/$m^2$.K) | T sol | T vis | E mis |
|---|---|---|---|---|---|---|
| PV-Window | Glass 1 (Low-Iron) | 0.003 | 1.114 | 0.91 | 0.91 | 0.840 |
| | PV Layer (a-Si) | 0.002 | 0.19 | 0.08 | 0.08 | 0.840 |
| | Air-Gap | 0.012 | 0.024 | | | |
| | Low-E Layer | 0.0047 | 1.000 | 0.68 | 0.83 | 0.158 |
| | Air-Gap | 0.012 | 0.024 | | | |
| | Glass 2 (Clear-Glz) | 0.003 | 1 | 0.83 | 0.9 | 0.84 |
| Clear-Window | Glass 1 (Low-Iron) | 0.003 | 1.114 | 0.91 | 0.91 | 0.840 |
| | Air-Gap | 0.012 | 0.024 | | | |
| | Low-E layer | 0.0047 | 1.000 | 0.68 | 0.83 | 0.158 |
| | Air-Gap | 0.012 | 0.024 | | | |
| | Glass 2 (Clear-Glz) | 0.003 | 1 | 0.83 | 0.9 | 0.84 |

### 2.4. Simulation model

The parametric design tool Rhinoceros (by McNeel & Associates) and its visual programming editor (Rutten, 2017), Grasshopper, were used to define the geometry and model the room. Various interactive 2D and 3D visual representations are provided by Ladybug which can be imported into Grasshopper to aid decision-making in the early phases of the design process (Sadeghipour Roudsari et al., 2013). Ladybug Tools, a validated tool (Taveres-Cachat & Goia, 2020), lets users take advantage of validated energy and daylighting engines such as EnergyPlus, Radiance, and Daysim.

***Table 4.*** *Overall window characteristics.*

| | PV_Win | Clear_Win |
|---|---|---|
| **U-factor (W/$m^2$. $K$)** | 1.36 | 1.39 |
| **T sol** | 0.04 | 0.52 |
| **SHGC** | 0.13 | 0.69 |
| **T vis** | 0.06 | 0.7 |

Radiance is a validated raytracing software that was described by (Subramaniam, 2022), was developed at the Lawrence Berkeley National Laboratory in the mid-1980s, and has been continued development since then. Empirical validation of Radiance for daylit spaces was published by (Mardaljevic, 1999) and corresponding validation for simulating artificially lit spaces was conducted by (Grynberg, 1989). Radiance through LBT (Mackey et al., 2017; Fang, 2017) is used to compute spherical view factors from each sensor to the surfaces of the model to determine longwave radiant temperatures. The view factor is the fraction of radiation leaving one surface and reaching the other surface directly (Hensen, 2019). Also, it is independent on the surface properties and temperatures (Subramaniam et al., 2022). To calculate the longwave MRT (Mean Radiant Temperature) at each sensor, the view factors are multiplied by the surface temperatures output by EnergyPlus through LBT, and the using method was validated by Mackey et al., 2017. It assumes that all indoor shades (e.g., those representing furniture) are at the room-average MRT (Menchaca-Brandan et al., 2017). For computing illuminance metrics, shortwave MRT calculations are needed. For all shortwave MRT calculations, LBT uses a radiance-based enhanced 2-phase method, which includes tracing a ray from each sensor to the solar position at each hour of the calculation to accurately represent the direct sun.

Outdoor air temperatures, relative humidities, and air speeds are taken directly from the EPW (Mackey et al., 2017). No obstructions outside the office, such as surrounding buildings and vegetation are assumed. Using EnergyPlus via LBT, light intensity is controlled according to natural daylighting, while a certain illumination is kept as a reference point. A daylight and thermal performance simulation requires the basic elements (Hensen, 2019):

- An optical material descriptions for all surfaces in the scene, the setup comprises a three-dimensional geometric model of the illuminated object(s).
- A sky model assesses the quantity of direct sunlight and diffuse daylight from various segments of the celestial hemisphere. Contemporary sky models employed in Daylight Coefficient simulations are rooted in Perez Skies (Subramaniam & Mistrick, 2017) with 145 patches of Tregenza subdivision (discourse.ladybug.tools).
- Space usage information such as working hours of an office space or the acceptable illuminance.
- An specific viewpoints or discrete sensors, such as a grid of illuminance sensors facing upwards to evaluate the amount of daylight.
- Calculating illuminance within the scene by the daylight simulation engine by combining the sky model with the scene.

Working hours for the Study office room are chosen from 7 am to 3 pm, and Thursday and Friday are defined holidays, according to the region's cal-

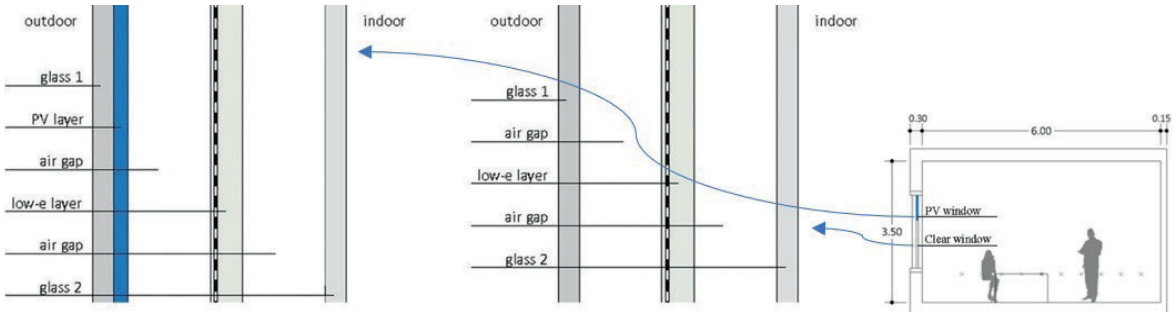


***Figure 2.*** *Schematical drawings of the PV window (left) and of the clear window (right), and schematical diagram of the office room.*

endar. An illuminance value of 300 lx is considered acceptable for working interiors (Chartered Institution of Building Services Engineers [CIBSE], 2005). To measure the daylight and thermal metrics, a grid of sensors with dimensions of 0.5x0.5 and a height of 0.7 meter is placed at a distance of 1 meter away from the window. This grid consists of a total of 90 points (figure 3). Additionally, an optional automatic dimming system is implemented to regulate artificial lighting. When the daylight at a reference point in the middle of the room reaches a specific illumination level of 300 lux, the system turns off the artificial lighting. Conversely, if the daylight falls below the set threshold, the artificial light adjusts dynamically to increase the light intensity within the room. (Associacao Brasileira de Normas Tecnicas [ABNT], 1992). This will result in a lower lighting consumption in the climates under review, considering high daylight availability of the cities. The values, thermal and visual performance metrics, are calculated for each of the 90 calculator points obtained and the average is studied.

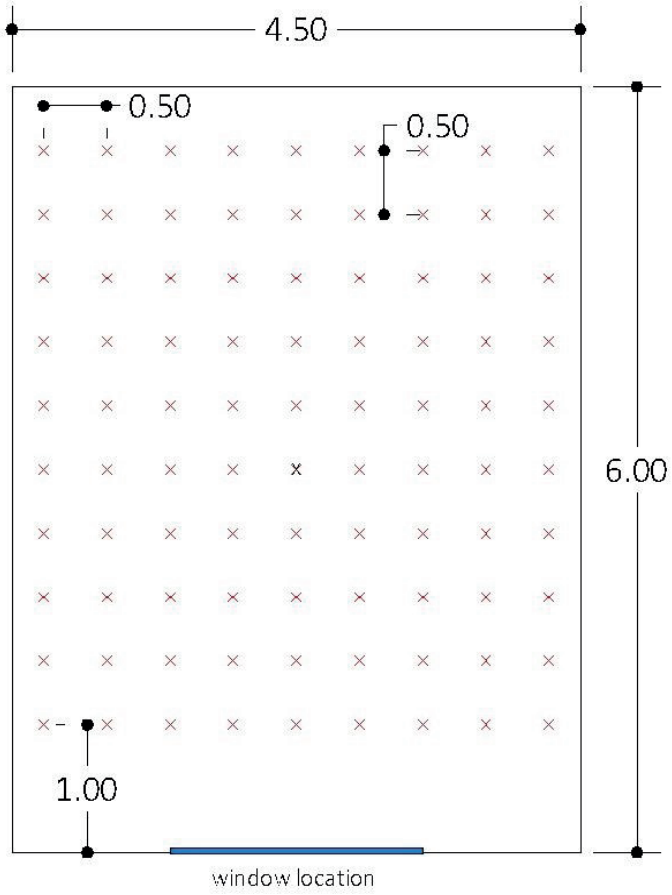


***Figure 3.*** *Reference point and grid of calculator points.*

To find the zone's annual and monthly energy consumption with EnergyPlus a fan coil with a gas heating unit is considered for the room. Setpoints are specified as 18 and 24 Celsius degrees. An air infiltration rate equal to 0.0003 $m^3/s.m^2$, the standard infiltration for an average building, is applied.

### 2.4.1. Electrical model

A method for calculating the electricity generated by a photovoltaic cell based on the anisotropic radiance distribution of incident solar radiation was applied. First, using simulation the diffuse solar radiation incident on the PV panels from the sky distribution was calculated, accounting for anisotropic effects. Next, we predict the PV panel's electricity production based on temperature by utilizing the linear expression proposed by Evans and Florschuetz (1977) (equation 1). By combining the incident radiation values with the temperature-dependent efficiency, we can model the quantity of electricity produced by the PV system under different weather conditions.

The quantities $T_{coeff}$ and $REF_{eff}$ are normally given by the PV manufacturer. In this workflow, they are assumed 0.2% and 5.2%, respectively (Didoné, Wagner, 2013). $T_{ref}$ assumed as 25 °C and the average of the outside window surface temperature and the inside window surface temperature that is calculated hourly via simulation specified as the cell temperature. The result of (equation 1) can then be multiplied by the area of the window (equation 2) to calculate the generated electricity (Didone & Wagner, 2013).

Equation 1 and equation 2 are added manually to the simulation model. The energy balance equations treated the test cell as a thermally isolated system made of a single homogeneous material, without considering changes in efficiency over time or explicitly modeling temperature-dependent loss mechanisms.

### 2.4.2. Thermal comfort model

To determine the thermal performance metric (TCP, the percentage of occupied time where thermal conditions are acceptable or comfortable [Annual]), the occupancy schedules of the energy model are considered.

$$PV_{eff} = REF_{eff} \times \left(1 + T_{coeff} \times (t - T_{ref})\right)$$

Where: $T_{coeff}$=The temperature coefficient of maximum power output for a-Si; $REF_{eff}$=Efficiency of PV module at the reference temperature; $T_{ref}$=Reference temperature; t=the cell temperature.

***Equation 1.*** *PV panel's electricity production.*

$$W = \mathrm{I} * (1 - \alpha) \times (1 - \rho) * \mathrm{PV}_{eff}$$

Where: α =glass absorption (0.012); ρ =and glass reflection (0.081); I =incident solar radiation (calculated for each hour via simulation)

***Equation 2.*** *Generated electricity.*

Occupied hours are determined from the occupancy schedules. In addition to model geometry, a sensor grids model is needed. It is what determine where the comfort mapping occurs. Predicting occupant thermal comfort involves considering factors such as air temperature, thermal radiation, humidity, and air speed. Thermal radiation refers to the release of electromagnetic waves from any substance with a temperature above absolute zero. It is the condition of mind that expresses satisfaction with the thermal comfort of the environment (ANSI/ ASHRAE Standard 55). The thermal comfort equation was established by P.O Fanger in the 1970s, penned as "Fanger's Comfort Equation". By employing Fanger's equation, we can determine a figure known as the Predicted Mean Vote (PMV), a metric that enables the prediction of the proportion of dissatisfied people (PPD). It has demonstrated remarkable accuracy. This provides a robust indication of how occupants in an area perceive the climate of their surroundings. The PMV model has become internationally accepted as a standard for describing the predicted mean thermal comfort of individuals within indoor environments. There is a strong correlation between thermal comfort and levels of productivity in offices, and in numerous instances, if temperature issues are not addressed within a reasonable time scale, can result in elevated staff turnover.

### 2.4.3. Visual comfort model

To determine the daylight performance metric UDI (Useful Daylight Illuminance represents the percentage of occupied hours that illuminance falls between a predefined range, 100 and 2000 lux in this study) was calculated. The strategy involves refining the metric by excluding summer periods between 7 am to 3 pm when interior daylight illuminances within the analysis area fall below 100 lux or surpass 2000 lux. These limits are chosen based on empirical evidence of occupant preferences in daylit offices equipped with user-operated shading devices (Konis, et al., 2016) that serve as the threshold criteria for the UDI metric developed by Nabil and Mardaljevic (2006). Specifically, it lowers the "sufficiency" threshold to 100 lux and incorporates a discomfort threshold of 2000 lux as an indicator of glare discomfort (Konis, et al., 2016). Therefore, in the ongoing study, the derived daylighting performance indicator is referred to as Useful Daylight Illuminance ($UDI_{100-2000}$).

### 2.4.4. Parametric study and fitness function

Heating energy demand is provided by gas in Iran so in the objective function, heating consumption was ignored. The total energy consumption is the result of cooling and lighting energy. Note that the cooling and lighting demand and electricity generation were calculated just for the hot period (21st June to 21st September).

The aim is to find the best PV-integrated window dimensions that can balance total building electricity demand and occupants' well-being through a multi-objective approach. useful daylight Illuminance (UDI) is analyzed to represent the occupant's visual comfort, and thermal comfort percentage (TCP) is investigated to show the thermal comfort of residents. Energy Saving (E_net) of the building as another goal was calculated considering electricity generation by the window, and cooling and lighting demand as electricity consumption (equation 3).

$$UDI + TCP - E\_net$$

$E\_net = Elec_{req} - Elec_{gen}$ ($Elec_{req}$ is more than $Elec_{gen}$, always)

$Elec_{gen}$ = total electricity generated by BIPV in the summer

$Elec_{req}$ = total energy consumption (cooling + lighting) in the summer

***Equation 3.*** *Generated electricity.*

$$F_{i=}(UDI_i - UDI_{min})C_1 + (TCP_i - TCP_{min})C_2 - (E_{net_i} - E_{net_{min}})C_3$$

Where:

i = result of iteration

Min = minimum value of optimization set

Max = maximum value of optimization set

$$C_1 = \frac{100}{UDI_{max} - UDI_{min}}$$

$$C_2 = \frac{100}{TCP_{max} - TCP_{min}}$$

$$C_3 = \frac{100}{E\_net_{max} - E\_net_{min}}$$

***Equation 4.*** *Fitness function.*

The three terms, UDI, TCP, and E-net, are contingent on the radiation entering the room which is dependent on the window area and its features. Cooling and lighting demand and electricity generated are the sum of normalized energy per unit conditioned floor area. This facilitates the comparison between them (Konis, et al., 2016). To find the fitness function with the best weight for each term, the weight-sum function method is utilized (equation 4). This method was introduced by (Konis, et al., 2016) and applied by (Pilechiha, et al., 2020) previously:

Note that here, three objectives are optimized and then the fitness function is calculated to rank the solution and conclude the best. Five values as WWR and seven values as PVWinR are investigated which resulted in 35 various states. After the optimization, using the genetic algorithm and Galapagos plugin via LBT, all outputs are transferred to an Excel file. The top model is selected among other options, using eq. 4.

## 3. Results and discussion according to climate regions and scenarios

### 3.1. Energy consumption and electricity generation

At the first step, the energy consumption and electricity generation of the cities are compared to provide an overview regarding the different climates. To this purpose, PV-window with 20% PV-integrated layer and with 80% PV-integrated layer is simulated. WWR considers 50% for both (Figure 4).

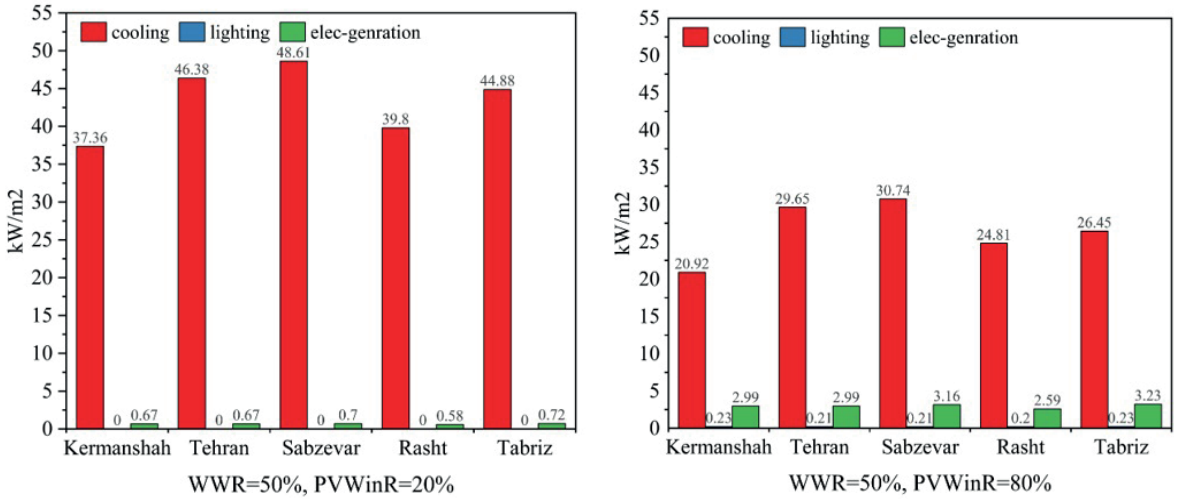


***Figure 4.*** *Energy performance with different window configurations.*

Figure 4 shows cooling consumption in Sabzevar is the highest amount and Kermanshah needs the least cooling demand among cities. The most figure of electricity generated occurs in Tabriz as it has a clear sky and is located in a higher elevation. Using a 50% WWR for the office room leads to no lighting demand if 80% of its area is specified as a clear window. Covering 80% of that with PV layers causes increasing lighting demand, but it, also, leads to less cooling consumption. Reduction in cooling demand is more notable. It is obvious that the more PV windows, the more electricity is generated.

The performance differences across climate zones reveals critical insights. Table 5 shows the details of the optimization, including UDI, TCP, E-net of each climate for each PV-window configuration. According to it, arid Climates show the highest E_net values at low PVWinR%, indicating greater energy demand, likely due to cooling loads and temperature fluctuation in these climates. However, it also demonstrates the most substantial energy savings from PV integration, with E_net reductions of up to 45% when comparing 0.2 to 0.8 PVWinR% at WWR 60%. This suggests that BIPV windows are particularly effective in arid climates with high solar radiation availability. Warm Temperate Climate (Rasht, Cfa) shows more moderate E_net values across all configurations compared to arid regions, but still demonstrates significant improvements with PV integration. The balance between heating and cooling seasons in this climate creates a more consistent performance profile across different WWR values.

### 3.2. Thermal comfort analysis

According to the Table 5, thermal comfort percentage decreases when WWR increases. The least amount of TCP is caused by the largest WWR when 80% of the window is comprised of clear glazing. In other words, when window ratio is high, covering it with PV layer can improve thermal comfort condition. For each WWR level, the largest TCP is experienced when the most of the window is PV integrated window. Increasing the PV covered area of the window is more influential in Theran and Sabzevar, hot climates, rather than other climates. For instance, Tehran shows a distinctive pattern where TCP values improve dramatically with increasing PVWinR%, especially at higher WWR values. At WWR 80%, TCP increases from 27.4% to 69.5% as PVWinR% increases from 0.2 to 0.8, suggesting that the semi-transparent PV effectively mitigates the excessive solar gain that would otherwise create thermal discomfort in this climate.

### 3.3. Visual comfort analysis

As the WWR increases from 20% to 80%, the UDI values generally improve across all cities, and it is because of the enhanced daylight availability. It is shown in Table 6 that larger window sizes contribute positively to achieving optimal daylight levels indoors. For instance, in Tehran (BSh semi-arid climate), UDI increases from approximately 45% at WWR 20% to 77-80% at WWR 80%, demonstrating that daylight availability significantly improves with larger fenestration in this climate zone due to the abundant clear sky conditions characteristic of semi-arid regions.

For each WWR level, increasing PVWinR generally does not have a significant impact on UDI values, with only minor variations observed as PV coverage changes from 0.2 to 0.8. This indicates that higher PV coverage ratios minimally affect the daylight performance. Overall, across all cities, the highest UDI values are observed with an 80% WWR, regardless of the PVWinR, suggesting that window size has a more significant impact on daylight availability than the PV coverage ratio. The consistent UDI values across PVWinR levels indicate that higher PV coverage does not substantially impair daylight access, making it feasible to integrate PV for energy generation without compromising daylight quality, particularly in regions with high solar exposure like cities investigated in this study (Table 5).

### 3.4. Fitness function for each WWR and PVWinR

Simulation is done for 25 different states of PV-integrated windows for all various climates and the outputs

***Table 5.*** *UDI, TCP, E-net of different BIPV windows.*

| WWR % | PVWinR | kermanshah | | | Tehran | | | Sabzevar | | | Rasht | | | Tabriz | | |
|---|---|---|---|---|---|---|---|---|---|---|---|---|---|---|---|---|
| | | UDI % | TCP % | E_net kWh/m2 | UDI % | TCP % | E_net kWh/m2 | UDI % | TCP % | E_net kWh/m2 | UDI % | TCP % | E_net kWh/m2 | UDI % | TCP % | E_net kWh/m2 |
| 20 | 0.2 | 45.0 | 88.6 | 20.5 | 45.7 | 84.4 | 27.1 | 45.8 | 85.0 | 28.0 | 46.1 | 83.0 | 23.0 | 47.3 | 83.6 | 24.8 |
| | 0.4 | 44.9 | 91.1 | 17.9 | 45.9 | 91.8 | 24.5 | 46.0 | 91.7 | 25.2 | 46.3 | 88.3 | 20.7 | 46.9 | 88.2 | 22.0 |
| | 0.5 | 45.1 | 91.7 | 17.0 | 46.0 | 93.2 | 23.5 | 45.9 | 93.0 | 24.2 | 46.4 | 90.5 | 19.9 | 47.2 | 89.6 | 20.9 |
| | 0.6 | 45.1 | 92.3 | 16.1 | 46.0 | 94.6 | 22.6 | 46.0 | 94.6 | 23.2 | 46.4 | 92.6 | 19.0 | 47.2 | 90.7 | 19.8 |
| | 0.8 | 45.1 | 92.1 | 16.7 | 45.8 | 96.8 | 23.0 | 46.2 | 96.6 | 23.3 | 46.4 | 95.1 | 19.6 | 47.5 | 91.1 | 19.6 |
| | | | | | | | | | | | | | | | | |
| 40 | 0.2 | 71.2 | 65.0 | 30.8 | 69.9 | 57.7 | 39.0 | 70.8 | 56.1 | 40.8 | 72.4 | 61.8 | 33.4 | 70.2 | 58.6 | 37.2 |
| | 0.4 | 71.2 | 74.7 | 25.7 | 70.2 | 65.8 | 33.8 | 70.8 | 65.5 | 35.2 | 72.3 | 70.0 | 28.8 | 69.6 | 67.7 | 31.5 |
| | 0.5 | 70.8 | 79.6 | 23.5 | 70.2 | 70.6 | 31.6 | 70.4 | 70.7 | 32.9 | 72.6 | 73.7 | 26.8 | 69.2 | 72.1 | 29.0 |
| | 0.6 | 70.7 | 84.9 | 20.6 | 70.1 | 78.8 | 28.6 | 70.0 | 79.2 | 29.7 | 71.9 | 79.3 | 24.1 | 70.1 | 78.5 | 25.8 |
| | 0.8 | 71.2 | 89.5 | 16.7 | 70.4 | 92.4 | 24.6 | 70.6 | 92.2 | 25.3 | 72.5 | 89.0 | 20.5 | 69.6 | 87.6 | 21.1 |
| | | | | | | | | | | | | | | | | |
| 50 | 0.2 | 77.1 | 53.9 | 36.7 | 76.1 | 47.9 | 45.7 | 76.0 | 45.6 | 47.9 | 78.5 | 51.3 | 39.2 | 74.8 | 47.4 | 44.2 |
| | 0.4 | 77.3 | 64.2 | 30.4 | 75.9 | 57.0 | 39.3 | 76.8 | 55.4 | 41.1 | 77.7 | 60.8 | 33.5 | 74.8 | 57.4 | 37.1 |
| | 0.5 | 77.0 | 71.1 | 26.7 | 76.4 | 62.3 | 35.6 | 76.1 | 62.2 | 37.2 | 78.1 | 66.9 | 30.2 | 74.7 | 63.4 | 33.1 |
| | 0.6 | 77.3 | 76.2 | 24.0 | 75.8 | 67.6 | 32.9 | 76.6 | 67.8 | 34.2 | 77.7 | 71.3 | 27.8 | 75.1 | 69.3 | 30.1 |
| | 0.8 | 77.8 | 86.7 | 18.2 | 75.7 | 85.2 | 26.9 | 76.9 | 85.7 | 27.8 | 77.8 | 82.7 | 22.4 | 74.7 | 82.4 | 23.4 |
| | | | | | | | | | | | | | | | | |
| 60 | 0.2 | 80.5 | 45.9 | 41.8 | 78.6 | 39.9 | 51.5 | 79.5 | 37.4 | 54.1 | 80.2 | 43.1 | 44.3 | 76.5 | 38.3 | 50.2 |
| | 0.4 | 80.5 | 56.4 | 34.2 | 78.8 | 49.6 | 43.9 | 79.4 | 47.7 | 46.0 | 80.3 | 53.4 | 37.5 | 76.7 | 49.4 | 41.8 |
| | 0.5 | 80.8 | 63.3 | 29.9 | 78.5 | 56.1 | 39.6 | 79.4 | 54.6 | 41.4 | 80.6 | 59.9 | 33.6 | 76.5 | 56.0 | 37.0 |
| | 0.6 | 80.8 | 69.1 | 26.7 | 78.6 | 60.9 | 36.3 | 79.5 | 60.7 | 37.9 | 80.6 | 65.4 | 30.7 | 76.7 | 61.7 | 33.4 |
| | 0.8 | 80.8 | 82.9 | 19.5 | 79.0 | 78.0 | 28.9 | 79.3 | 78.6 | 30.0 | 80.5 | 78.0 | 24.1 | 76.7 | 77.6 | 25.4 |
| | | | | | | | | | | | | | | | | |
| 80 | 0.2 | 80.4 | 33.6 | 50.2 | 77.8 | 27.4 | 61.4 | 78.1 | 25.2 | 64.7 | 80.3 | 32.0 | 52.9 | 75.7 | 27.4 | 60.3 |
| | 0.4 | 80.5 | 45.3 | 40.3 | 77.7 | 38.7 | 51.5 | 78.1 | 36.4 | 54.1 | 80.4 | 42.6 | 44.0 | 75.7 | 37.0 | 49.4 |
| | 0.5 | 80.5 | 50.4 | 36.1 | 77.7 | 44.3 | 47.2 | 78.2 | 42.1 | 49.5 | 80.4 | 47.8 | 40.1 | 75.6 | 42.8 | 44.7 |
| | 0.6 | 80.4 | 59.2 | 30.4 | 77.8 | 51.8 | 41.5 | 78.2 | 50.0 | 43.5 | 80.3 | 56.0 | 35.0 | 75.6 | 51.8 | 38.4 |
| | 0.8 | 80.5 | 75.9 | 20.7 | 77.8 | 69.5 | 31.5 | 78.2 | 69.2 | 32.9 | 80.4 | 71.1 | 26.2 | 75.7 | 70.4 | 27.6 |

are transferred to an Excel file. Using equation 4, the result of F as the fitness function, representative of UDI, TCP, and energy saving, is calculated for each PV percentage and WWR (Figure 5). The trend is similar for cities and with specifying PVWinR as 80% while WWR is 50 percent, the highest amount of F is obtained.

Figure 5 illustrates that when WWR is 20%, increasing the PV share of the window from 80 to 60 percent resulted in decreasing F. It means if the share of the window area is small, specifying at least 40% of that as a clear window is important for the workflow's purposes. The effect of the PV layer grows as WWR increases as far as in the case WWR=80%, there is a dramatic difference between PVWinR as 20% and 80%, equal to roughly 200. When a large window ratio is selected while 80% of its area is a clear window with a U-value equal to 1.3, it may cause no thermal comfort. A large WWR leads to more heat transfer and energy consumption. The best solution of this parametric study is a window ratio of 50% of the south wall and a PV ratio of 80% of the window area (Figure 5).

In all cases, Kermanshah and Tabriz comprised the largest amount of F which means providing higher UDI, TCP, and lower energy consumption is easier than other cities. Tehran and Sabzevar peaked at the lowest figure of F. Among the climates shown, Rasht has the highest humidity rate and a cloudy sky.

### 3.5. Payback of the BIPV glazing system

The average price for a European BIPV glass-glass module is about 120-250€/m2, whereas the minimum price for a European standard glass-glass module can be as low as 95€/m2. The cost can go up to 380€/m2 if you want a unique solar exterior customization (Metsolar, 2022). According to the National Renewable Energy Laboratory (NREL), the cost of different layers of windows is considered. Air space between glazing, frame for the window, wiring to connect the PV cells to an inverter, and installation cost aren't taken into account. The price of different layers is presented in Table 6 (Pvinsights,

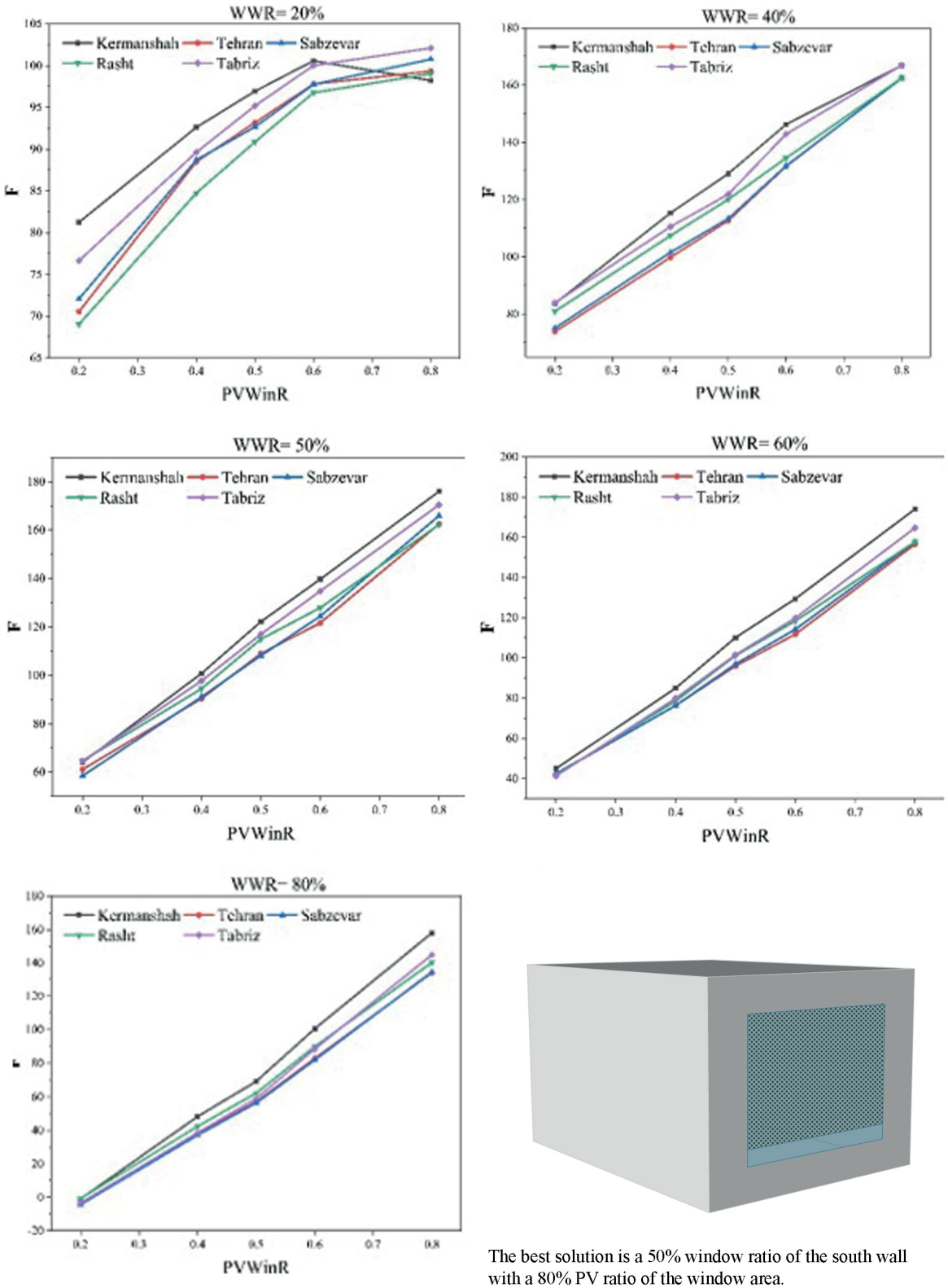


***Figure 5.*** *Comparison F as the fitness function for various WWR and PVWinR and the best configuration.*

March 2023). The maximum power of the BIPV window is defined as 300 watts.

According to figure 6 the best solution of this parametric study is a window ratio of 50% of the south wall and a PV ratio of 80% of the window area. So, the height and width of the window is 1.9 m and a 3.2 m, respectively. The upper part of that is PV-integrated which means a 1.52 x 3.2 PV window. Thus, the area of the PV-integrated window is 4.864, and of the clear window is 1.216 square meters (Table 7).

Electricity prices are studied in 100 countries (globalpetrolprices, 2022) and the world average price is 0.164 U.S. Dollars per kWh. Considering 6 sunshine hours for all days and the PV panel with 5.2% efficiency and 4.864 square meter area, the electricity generation is obtained 1329 kilo Watt annually.

This leads to 217.9$ in saving money each year. Therefore, using Simple Payback Period method, the payback of the BIPV window system would be approximately 16 months. There are, also, some incentives that governments usually offer to generate energy using renewable resources and to reduce greenhouse gas emissions (Table 7).

## 4. Conclusion

This paper proposed a framework for using a PV layer between triple-glazing windows. The result of electricity demand, and thermal and visual comfort of both a PV window and a clear window with the same U-value for an office room was investigated using EnergyPlus and Radiance via Ladybug Tools. The properties of the windows were modeled through the window tool from Berkeley Lab. Various ratios were studied as the window-to-wall ratio and the PV-area-to-Window ratio.

The PV-area-to-Window demonstrates an interesting relationship with performance metrics. As PVWinR% increases from 0.2 to 0.8:

- UDI remains relatively stable or slightly decreases at higher PVWinR% values. This suggests that while PV integration reduces visible light transmittance, the effect on useful daylight is minimal.
- TCP shows a clear positive correlation with increasing PVWinR%, most pronounced in all climate zones at higher WWR values. This improvement can be attributed to the PV elements providing shading that reduces solar heat gain, particularly critical in arid climates with high solar radiation.
- E_net consistently decreases with increasing PVWinR%, demonstrating the energy generation benefit of PV integration. Cooling consumption decreases because of the lower SHGC of PV window rather than of a clear window. As a result, an impressive reduction occurs in energy consumption. It means at higher PVWinR electricity demand decreases.

Using a total PV window leads to more savings in studied different climates, but increasing WWR significantly affects fitness function which represents UDI, TCP, and energy consumption. Also, PV share affects the study goals significantly when WWR is specified as more than 40%. Optimizing the performance of a large window is accessible using the BIPV window. For all regions, applying a window with a higher percentage of PV will result in more electricity saving, thermal comfort, and useful daylight illuminance.

The complex interrelationships between WWR, PVWinR%, and performance metrics across different climates suggest that optimization must be climate-specific:

- In arid and semi-arid climates, higher PVWinR% values (0.6-0.8) paired with moderate WWR (40-60%) appear to offer the best balance of daylight, thermal comfort, and energy performance.
- In the warm temperate climate, Rasht, a more moderate approach with WWR around 40-60% and PVWinR% of 0.4-0.6 provides optimal balance.

***Table 6.*** *Windows layers' price.*

| | Low-iron glass ($ per $m^2$) | Encapsulated film ($ per $m^2$) | Back-shit film ($ per $m^2$) | Low-E coated glass ($ per $m^2$) | Clear glass ($ per $m^2$) | Thin film module ($ per Watt) | BIPB window power (W) | Area ($m^2$) | Total Price |
|---|---|---|---|---|---|---|---|---|---|
| | 16.4 | 7 | 8 | 10-25 (17.5) | 1-10 (5) | 0.21-0.31 (0.26) | 300 | - | - |
| Clear window | + | | | + | + | | | 1.216 | 47 |
| PV-window | + | + | + | + | + | + | | 4.864 | 340 |

***Table 7.*** *Payback time.*

| | sunshine hours | efficiency | PV window area ($m^2$) | electricity generation (kW/year) | Electricity prices ($ per kWh) | saving money ($ per year) |
|---|---|---|---|---|---|---|
| | 6 | 5.2 | 4.864 | 1329 | 0.164 | 217.9 |
| Payback Time | 16 months | | | | | |

These findings underscore that BIPV window design must consider the specific solar radiation patterns, seasonal temperature variations, and daylight characteristics of each climate zone rather than applying universal design guidelines.

The present study's findings demonstrate notable alignment with several previous research outcomes while also revealing some distinct variations. Similar to Chen et al. (2019), our results confirm that PV windows significantly reduce cooling energy consumption, though our optimal WWR of 40-60% differs from their recommended 83%. This variance likely stems from our holistic approach incorporating comfort metrics alongside energy performance. Our findings of achieving optimal performance (F value of 120-140) with 60% PV coverage at lower WWRs (40-60%) presents a more balanced solution compared to Chen's recommendation of 87% PV coverage. These results align more closely with Sun et al. (2020) and Liu et al. (2019), who emphasized the importance of balanced daylight and glare control. The thermal conductivity of our tested window (0.04 W/(m.K)) matches Chen et al.'s (2019) findings, validating the thermal performance aspects. Furthermore, while Kim et al. (2023) focused primarily on energy generation potential for NZB buildings, our study expands on their framework by incorporating comfort metrics, demonstrating that optimal energy performance can be achieved without compromising occupant comfort. The observed improvement in daylight uniformity and glare reduction aligns with Hu et al.'s (2023) findings regarding CdTe windows, though our study employs different PV technology (a-Si cells) and achieves comparable performance improvements. Numerous parameters influence the results obtained in this study and similar research, and the extent of each parameter's impact on the overall outcome remains undetermined, direct comparisons between studies require aligning multiple variables. These variables may include building type (residential, commercial, etc.), photovoltaic panel specifications, and other contextual factors. However, achieving such alignment is often impractical due to the diversity of study conditions. Therefore, the findings of this research should be interpreted independently, allowing readers to assess their relevance based on specific contextual similarities.

In this study, a Window Integrated Photovoltaic (WIPV), was proposed to offer simultaneous improvement of daylighting control, thermal comfort, on-site electricity generation, and energy consumption. Providing energy demand via renewable resources that result in less pollution is one of the main purposes of utilizing such technologies which improves the energy saving of a building (capital of such solar windows is returnable and it is economically justifiable).

In the future, investigating other kinds of PV cells can be worked on to find the most economical and efficient combination of a BIPV window. Also, state-of-the-art window technologies such as the insulating glass unit (IGU) are proposed widely which can be investigated. The framing material can significantly impact the U-value of a window which is not studied in this paper. Finally, a comparison between PV-integrated shading that can optimize useful daylight and thermal comfort can be the future research.

**Endnotes**

[1] Window-to-Wall Ratios.

[2] Useful Daylight Illuminance.

**Acknowledgment**

The authors want to express their sincere gratitude to Hamid Montazeri and to Rima Fayaz for the time they generously allocated and for the support they provided, which was instrumental in helping the authors complete this article and to Abolfazl Ganji Kheybari who helped advance this research. Their contributions were greatly valued and appreciated.

**References**

Associacao Brasileira de Normas Tecnicas (ABNT). (1992). NBR-5413: Iluminância de Interiores. *Rio de Janeiro,* 13p.

ANSI/ASHRAE. (2017). Standard 55: Thermal Environmental Conditions for Human.

Attoye, D.E., Tabet Aoul, K.A., Hassan, A. (2017). A Review on Building

Integrated Photovoltaic Façade Customization Potentials. *Sustainability, 9*(12), 22-87. https://doi.org/10.3390/su9122287

Bakmohammadi, P., Noorzai, E. (2021). Investigating the optimization potential of daylight, energy, and occupant satisfaction performance in classrooms using innovative photovoltaic integrated light shelf systems. *Science and Technology for the Built Environment, 4*(28), 467-482. https://doi.org/10.1080/23744731.2021.2014247

Cannavale, A., Ierardi, L., Hörantner, M., Eperon G.E., Snaith, H.J., Ayr, U., Martellotta, F. (2017). Improving energy and visual performance in offices using building integrated perovskite-based solar cells: A case study in Southern Italy. *Applied Energy, 205*, 834-846. https://doi.org/10.1016/j.apenergy.2017.08.112

Chae, Y.T., Kim, J., Park, H., Shin, B. (2014). Building energy performance evaluation of building integrated photovoltaic (BIPV) window with semi-transparent solar cells. *Applied Energy, 129,* 217-227. https://doi.org/10.1016/j.apenergy.2014.04.106

Chartered Institute of Building Services Engineers (CIBSE) (2005). *Lighting Guide 7: Office lighting.*

Chen, M., Zhang, W., Xie, L., Zhichun, N., Wei, Q., Wang, W., Hao, T. (2019). Experimental and numerical evaluation of the crystalline silicon PV window under the climatic conditions in southwest China. *Energy, 183,* 584-598. https://doi.org/10.1016/j.energy.2019.06.146

Didoné, E.L., Wagner, A. (2013). Semi-transparent PV windows: A study for office buildings in Brazil Evelise. *Energy and Buildings, 67,* 136–142. https://doi.org/10.1016/j.enbuild.2013.08.002

Do, S.L., Shin, M., Baltazar, J.C., Kim, J. (2017). Energy benefits from semi-transparent BIPV window and daylight-dimming systems for IECC code-compliance residential buildings in hot and humid climates. *Solar Energy 155,* 291-303. *https://doi.org/10.1016/j.solener.2017.06.039*

Evans, D.L., Florschuetz, L.W. (1977). Cost studies on terrestrial photovoltaic power systems with sunlight concentration. *Solar Energy, 19*(3), 255–262. https://doi.org/10.1016/0038-092X(77)90068-8

Fang, Y. (2017). *Optimization of Daylighting and Energy Performance Using Parametric Design*, *Simulation Modeling, and Genetic Algorithms.* [Doctoral dissertation, UC Berkeley, North Carolina State University]. UA Campus Repository. https://escholarship.org/uc/item/2zs2h81m

Gao, Y., Li, S., Fu, X., Dong, W., Lu, B., Li, Z. (2020). Energy management and demand response with intelligent learning for multi-thermal-zone buildings. *Energy, 210,* Article 118411. https://doi.org/10.1016/j.energy.2020.118411

Gentile, N., Lee, E.S., Osterhaus, W., Altomote, S., Naves David Amorim, C., Ciampi, G., Garcia-Hansen V., Maskarenj, M., Scorpio, M., Sibilio, S. (2022). Evaluation of integrated daylighting and electric lighting design projects: lessons learned from international case studies. *Energy and Buildings, 268,* Article 112191. https://doi.org/10.1016/j.enbuild.2022.112191

Ghosh, A., Sarmahb, N., Sundarama, S., Mallicka, T.K. (2019). Numerical studies of thermal comfort for semi-transparent building integrated photovoltaic (BIPV)-vacuum glazing system. *Solar Energy, 190*, 608-616. https://doi.org/10.1016/j.solener.2019.08.049

Global Solar Atlas. (2019). World Bank and International Finance Corporation, https://globalsolaratlas.info/

Globalpetrolprices. (2022). Electricity prices. https://www.globalpetrolprices.com/electricity_prices/

Grynberg, A. (1989). Validation of Radiance. Lawrence Berkeley Laboratory, Lighting Systems Research Group.

Hensen, J.L., Lamberts, R. (2019). *Building performance simulation for design and operation*, (2nd ed.). Routledge (Taylor & Francis Group).

Hu, Y., Xue, Q., Wang, H., Zou, P.,Yang, J., Chen, S., Cheng, Y. (2024). Experimental investigation on indoor daylight environment of building with Cadmium Telluride photovoltaic window. *Energy and built environment, 5*(3), 404-413. https://doi.org/10.1016/j.enbenv.2023.01.001

International Energy Agency (IEA). (2021). World Energy Balances. IEA,

Paris. Licence: Terms of Use for Non-CC Material. https://www.iea.org/data-and-statistics/data-product/world-energy-balances.

International Energy Agency (IEA). (2022, March 26). Energy Explained: Electricity, IEA. https://www.eia.gov/energyexplained/electricity/electricity-in-the-us.php

Kim, S., An, J., Choi, H., Hong, T. (2023). Assessment the technical and economic performance of a window-integrated PV system using third-generation PV panels. *Energy and Buildings, 286,* Article 112978. https://doi.org/10.1016/j.enbuild.2023.112978.

Konis, K., Gamas, A., Kensek, K. (2016). Passive performance and building form: An optimization framework for early-stage design support. *Solar Energy, 125,* 161-179. https://doi.org/10.1016/j.solener.2015.12.020

Kuhn, T.E., Erban, C., Heinrich, M., Eisenlohr, J., Ensslen, F., Neuhaus, D.H. (2021). Review of technological design options for building integrated photovoltaics (BIPV). *Energy and Buildings. 231*(5), Article 110381. https://doi.org/10.1016/j.enbuild.2020.110381

Liu, D., Sun, Y., Wilson, R., Wu, Y. (2019). *Comprehensive evaluation of windows integrated semi-transparent PV for building daylight performance*. Renewable Energy. 145, 1399-1411. https://doi.org/10.1016/j.renene.2019.04.167.

Liu, X., Wu, Y. (2022). Numerical evaluation of an optically switchable photovoltaic glazing system for passive daylighting control and energy-efficient building design. *Building and Environment, 219,* Article 109170. https://doi.org/10.1016/j.buildenv.2022.109170

Mackey, C., Baranova, V., Petermann, L., Alejandra, M. (2017). *Glazing and Winter Comfort, Part 2: An Advanced Tool for Complex Special and Temporal Conditions*. International Building Performance simulation association [2017 Building Simulation Conference]. https://doi.org/10.26868/25222708.2017.682

Menchaca-Brandan, M.A., Baranova, V., Petermann, L., Koltun, S., Mackey, C. (2017). *Glazing and Winter Comfort, Part 1: An Accessible Web Tool for Early Design Decision-Making. International Building Performance Simulation Association*. [15th IBPSA Conference presentation]. https://doi.org/10.26868/25222708.2017.688

Metsolar, (2022). *How much does really BIPV cost?*, EU manufacturer of solar modules. https://metsolar.eu/blog/how-much-does-really-bipv-cost/

*Mardaljevic, J. (1999). Daylight Simulation: Validation, Sky Models and Daylight Coefficients. [Doctoral dissertation, De Montfort University: Leicester, UK]*

Nabil, A., Mardaljevic, J. (2006). Useful daylight illuminances: a replacement for daylight factors. *Energy Building, 38*(7), 905-913. *https://doi.org/10.1016/j.enbuild.2006.03.013*

Nasrollahzadeh, N. (2021). Comprehensive building envelope optimization: Improving energy, daylight, and thermal comfort performance of the dwelling unit. *Journal of Building Engineering, 44,* Article 103418. *https://doi.org/10.1016/j.jobe.2021.103418*

Parida B., Iniyan S., Goic R. (2011). A review of solar photovoltaic technologies. *Renewable Sustainable Energy Reviews, 15*(3), 1625-1636. https://doi.org/10.1016/j.rser.2010.11.032.

Pilechiha, P., Mahdavinejad, M., Pour Rahimian, F., Carnemolla, P., Seyedzadeh, S. (2020). Multi-objective optimisation framework for designing office windows: quality of view, daylight and energy efficiency. *Applied Energy, 261,* Article 114356. https://doi.org/10.1016/j.apenergy.2019.114356

Pvinsights, (2023). *Solar PV Module Weekly Spot Price*, PVinsights.com. http://pvinsights.com/index.php

Roshan, Gh.R., Orosa, J.A., Nasrabadi, T. (2012). Simulation of climate change impact on energy consumption in buildings, case study of Iran. *Energy Policy, 49,* 731-739. https://doi.org/10.1016/j.enpol.2012.07.020.

Rutten, D. (2017, October 9). Grasshopper - Algorithmic Modeling for Rhino: version 0.9.0076. http://www.grasshopper3d.com/

Sadeghipour Roudsari, M., Pak, M., Smith, A., Gill, G. (2013). Ladybug: A parametric environmental plugin for Grasshopper to help designers create an environmentally-conscious design. [13th IBPSA Conference presentation], Chambery, France.

Samanoudy, G., Abdelaziz Mah-

moud, N.S., Jung, C. (2024). Analyzing the effectiveness of building integrated Photovoltaics (BIPV) to reduce the energy consumption in Dubai. *Ain Shams Engineering Journal, 15*(5), Article 102682. https://doi.org/10.1016/j.asej.2024.102682

Somasundaram, S., Chong, A., Wei, Z., Thangavelu, S.R. (2020). Energy saving potential of low-e coating based retrofit double glazing for tropical climate. *Energy and Buildings, 206,* Article 109570. https://doi.org/10.1016/j.enbuild.2019.109570

Subramaniam, S., Mistrick, R.G. (2017). *A More Accurate Approach for calculating Illuminance with Daylight Coefficients*. [The IES Annual Conference], Portland, Oregon, USA. https://www.researchgate.net/publication/325248556

Subramaniam, S., Hoffmann, S., Thyageswaran, S., Ward, G. (2022). Calculation of View Factors for Building Simulations with an Open-Source Raytracing Tool. *Applied Science, 12,* 27-68. https://doi.org/10.3390/app12062768.

Sun, Y., Liu, D., Flor, J.F., Shank, K., Baig, H.,Wilson, R., Liu, H., Sundaram, S., Mallick, T.K., Wu, Y. (2020). Analysis of the daylight performance of window integrated photovoltaics systems. *Renewable Energy, 145,* 153-163. https://doi.org/10.1016/j.renene.2019.05.061

Taşer, A., Kazanasmaz, Z. T. (2023). *Daylight Performance and Lighting Energy Savings of Amorphous and Crystalline Silicon Solar Cells in an Architecture Studio*. [IEEE International Conference on Environment and Electrical Engineering and 2023 IEEE Industrial and Commercial Power Systems Europe (EEEIC / I&CPS Europe)], Spain. https://doi.org/10.1109/EEEIC/ICPSEurope57605.2023.10194820.

Taveres-Cachat, E., Goia, F. (2020). Co-simulation and validation of the performance of a highly flexible parametric model of an external shading system. *Building and Environment, 182,* 107-111. https://doi.org/10.1016/j.buildenv.2020.107111

Yu, G., Yang, H., Luo, D., Cheng, X., Ansah, M. (2021). A review on developments and researches of building integrated photovoltaic (BIPV) windows and shading blinds. *Renewable and Sustainable Energy Reviews, 149*(1), Article 111355. https://doi.org/10.1016/j.rser.2021.111355